

Decoding and Mapping of Right Hand Motor Imagery Tasks using EEG Source Imaging

Brad Edelman, *IEEE Student Member*, Bryan Baxter, *IEEE Student Member*, Bin He, *IEEE Fellow*

Abstract— Current EEG based brain computer interface (BCI) systems have achieved successful control in up to 3 dimensions; however, the current sensor-based paradigm is not well suited for many rehabilitative and recreational applications that require motor imagination (MI) tasks of fine motor movements to be recognized. Therefore there is a great need to find complex MI tasks that are intuitive for BCI users to perform and that can be classified with high accuracy. In this paper we present our results on classifying four MI tasks of the right hand, flexion, extension, supination and pronation using a novel EEG source imaging approach. Using this approach we were able to improve the four-class classification of the four tasks by nearly 10% as compared to traditional sensor-based techniques.

I. INTRODUCTION

Non-invasive brain-computer interfaces (BCIs) utilizing sensorimotor rhythms (SMRs) determine a user's intent by identifying electroencephalographic (EEG) signals unique to different motor tasks. Motor imagery (MI), or the imagination of a particular movement, induces dynamic spectral-temporal activity within the primary motor cortex (M1) such that recording electrodes can detect which task is being performed. Control of real and virtual objects using MI paradigms have shown that these signals are reliable across multiple subjects and can be used for the successful operation of an SMR BCI in up to three dimensions [1,2].

Despite such achievements, the progress of these systems is limited by the low signal-to-noise ratio of scalp recorded EEG. The topographic organization of M1 dedicates control of different body parts to specific regions along the homunculus. Signal variation in the spatial domain should therefore allow for the recognition and separation of different MI tasks, however, signals collected by the scalp electrodes are known to be smeared representations of true cortical activity due to the volume conduction effect [3]. Therefore, the imagined movement of body parts which map to nearby cortical patches often produce similar patterns as detected on the scalp.

For many high dimension SMR BCIs, a solution is to simply employ MI tasks which activate distant areas of M1, such as the right and left hand, feet, and tongue. However, these tasks can be difficult to perform and are often irrelevant to both rehabilitative and recreational applications

of BCIs. Therefore, there is a great need to discover new techniques that are able to exploit tasks that can successfully be used to help regain fine motor control or achieve more realistic movement of output devices. For example, using foot/tongue MI tasks to control the trajectory or actions of a robotic arm is not intuitive. On the contrary, controlling a robotic arm by imagining the same action of a one's own arm/hand is more natural.

Nevertheless, few studies have examined the separability of MI tasks involving varying manipulations of the hand and often utilize complex signal processing techniques with inconsistent results [4–6]. EEG source imaging (ESI) is a spatial filtering technique that reconstructs the cortical current density (CCD) such that activity of anatomically relevant structures can be examined. ESI has gained popularity in the BCI community over the past decade with promising results [7–10] and may provide a means to separate MI tasks in source space that are more appropriate for intuitive control of SMR BCIs. In the present study we have investigated the ability to successfully discriminate between four MI tasks of the right hand, flexion, extension, supination and pronation. We hypothesized that the source space reconstruction of the MI activity would allow us to decode the four MI tasks with higher accuracy compared to the scalp EEG.

II. EXPERIMENTAL SETUP AND DESIGN

A. Motor Imagery Task

3 human subjects participated in this study by consenting to a protocol approved by the IRB of the University of Minnesota. Subjects were seated in front of a computer screen and instructed to perform 2Hz self-paced MI of right hand flexion, extension, supination or pronation (**Fig. 1a**). Flexion and extension, and supination and pronation MI tasks were paired together and randomized within each run. Each session was composed of four runs of 20 trials for each pair of tasks. Prior to the MI runs, subjects performed motor execution runs of the same tasks to prime their motor circuits and help mentally prepare for MI.

Trials were structured as outlined in **Fig. 1b**; a “rest” icon appeared on the screen for three seconds, followed by three seconds of a target indicating which MI task to perform. Finally, a four second “go” cue was presented during which the subject continuously performed the specified MI task. 64-channel EEG was acquired according to the standard 10-20 electrode system using a SynAmpsRT amplifier (Neuroscan Compumedics) at a sampling frequency of 1000Hz.

This work was supported in part by CBET-1264782, NSF DGE-1069104, and NIH R01 EB006433.

B. Edelman and B. Baxter are with the Department of Biomedical Engineering, University of Minnesota, Minneapolis, MN 55455, USA

B. He is with the Department of Biomedical Engineering and Institute of Engineering in Medicine, University of Minnesota, Minneapolis, MN 55455, USA

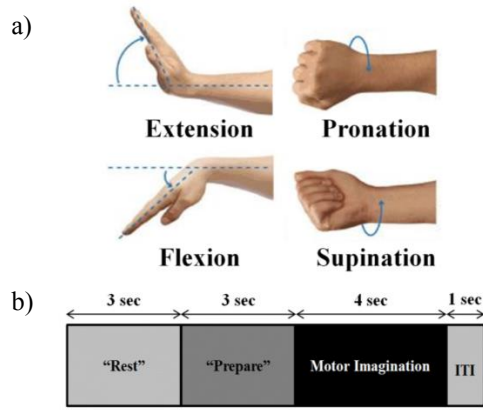


Fig. 1. (a) The four MI tasks the subjects performed. Subjects performed motor execution runs of the same tasks prior to the motor imagery runs. (b) Standard trial structure for the MI tasks. Each run contained 20 trials of each pair of tasks (flexion/extension or pronation/supination). Trials were randomized within runs.

B. EEG Preprocessing

Recorded data from all MI tasks were separated into four independent data sets and preprocessed in MATLAB. 17 electrodes overlying the motor cortex were utilized for this analysis. EEG recordings from these electrodes were band pass filtered between 8 and 30 Hz and trials containing artifactual behavior were removed by visual inspection. A surface Laplacian was then applied to the remaining trials to enhance focal activity of the MI task. Only the data from one second before the task started to one second after the task ended was kept for further analysis while the rest periods were discarded.

C. Weighted Minimum Norm Estimate

In order to bring the scalp-recorded potentials into source space the EEG inverse problem must be solved. The current density on the cortical surface can be computed by incorporating the brain's anatomical geometry and the electrical conductance of different cerebral tissues. The weighted minimum norm estimate (WMNE) finds the optimal source distribution, \hat{x} , by minimizing the residual between the recorded and estimated scalp potentials under a minimum energy constraint, as depicted in (1). In this equation, A represents the lead field, b the recorded scalp data, x the source distribution, W a weighting matrix, and λ a regularization parameter.

$$\min_x \|Ax - b\|_2^2 + \lambda \|Wx\|_2^2 \quad (1)$$

(1) can be solved for analytically to generate the closed-form solution (2).

$$\hat{x} = A^T(AA^T + \lambda W)^{-1}b \quad (2)$$

D. ROI Selection

To find a right hand cortical patch containing the overlapping origin from all four MI tasks, the individual task data were compiled into a single set. Independent component analysis (ICA) was then used to decompose the compiled, preprocessed data into temporally independent sources

within the EEG space. The independent component (IC) that displayed activation in electrodes overlying the left motor cortex and the event-related desynchronization (ERD) characteristic of motor processing [11] was selected as the source responsible for the total right hand MI activity. The chosen IC electrode topography was mapped onto a standard cortex template using the WMNE [12] to find dipoles belonging to the ROI. ROIs for the three subjects are presented in Fig 2.

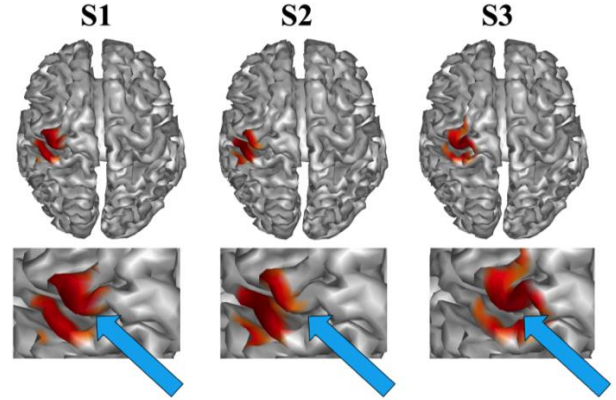


Fig. 2. The right hand ROI for each of the three subjects localizes to the left sensorimotor cortex. In each case the ROI incorporates the “hand knob” of the precentral gyrus.

E. Feature Extraction and Selection

Each of the four preprocessed MI data sets was mapped onto a standard cortex model using the WMNE for all selected time points. Waveforms from each dipole within the aforementioned ROI were convolved with a Morlet wavelet to obtain their time-frequency representation (TFRs). TFRs were broken into time windows and frequency bands that maximized classification accuracy.

The most discriminable features were found using the Mahalanobis distance (MD) in an iterative search method described in [13]. The MD (3) is a statistical measure of similarity between two distributions based on their respective mean, μ and pooled covariance, Σ .

$$d^2 = (\mu_1 - \mu_2)\Sigma^{-1}(\mu_1 - \mu_2)^T \quad (3)$$

The MD, however, is best suited for binary comparisons and therefore a one-vs-all approach was applied to each of the four MI tasks. By doing so, we were able to identify and rank spectral-temporal-spatial features that were most distinct to each task. The top features of each task were concatenated together and extracted from all four task data sets for classification.

F. Classification

A MD-based classifier was used for classification analysis. A 10-fold cross validation procedure was implemented using 90% training and 10% testing sets. This classifier was constructed by first finding the mean, μ_i , and covariance, Σ_i , of each of the four classes. The multivariate distance between each testing sample and the distribution of each task was computed in a similar fashion to (3). The

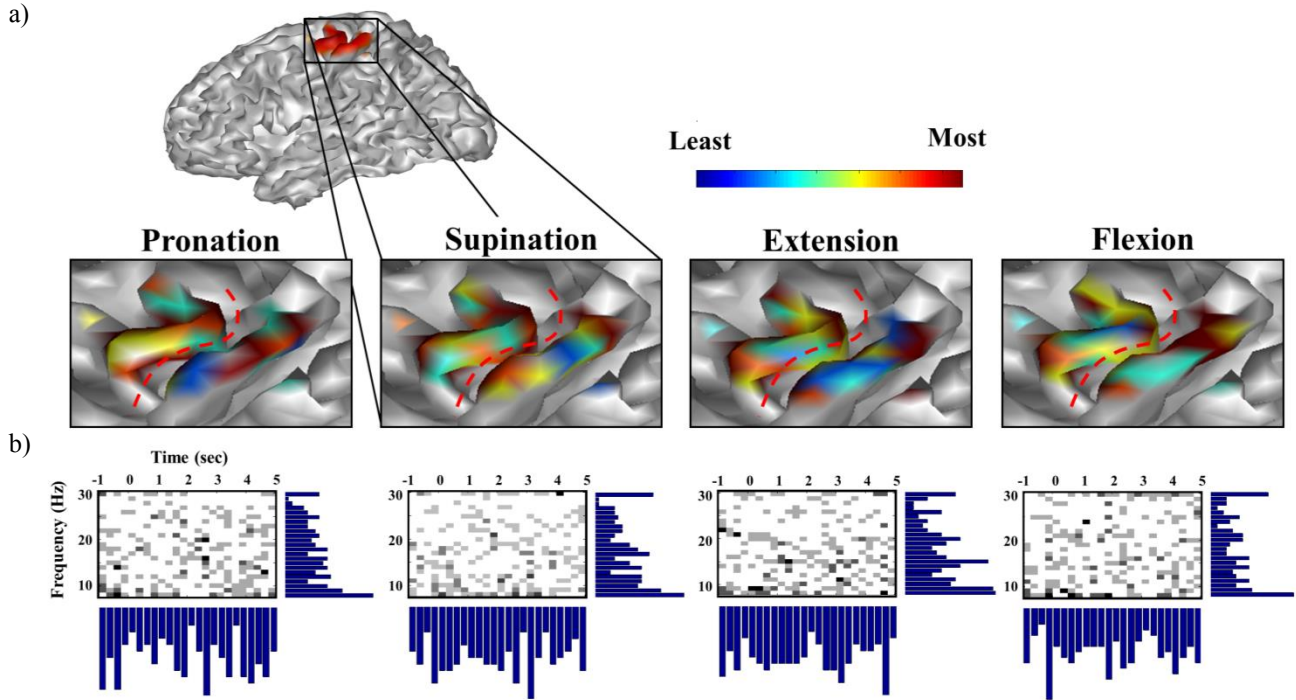


Fig. 3. (a) Spatial source-based feature maps within the right hand ROI (left motor cortex) of the most discriminable features for each of the four MI tasks. Warm colors indicate those dipoles that most contribute to the unique EEG traces of the corresponding MI task, whereas cool colors indicate low contribution. The central sulcus is indicated by the red dotted line. (b) Time-frequency feature maps indicating the spectral and temporal origin of the same features. Histograms below and to the right of the TFR maps display the distribution of features within the respective domain.

sample was ultimately assigned to the class that minimized the distance.

Classification accuracy was computed by dividing the number of correctly identified samples by the total number of testing samples. This was performed for the testing samples of each task as well as the entire testing set. The same analysis was performed on all sensor waveforms to compare the separability of these MI tasks between sensor and source space. For source space, the most discriminable features were traced back in time, space, and frequency to identify the unique distribution of each task in the respective domains.

III. RESULTS

A. Feature Mapping

Spatial source-based feature maps for each of the four MI tasks for subject 1 are displayed in **Fig. 3a**. Warm colors indicate those dipoles which most contribute to the unique characteristics of the indicated task, whereas cool colors indicate those dipoles which contribute less. Features were also traced back in the spectral and temporal domains and are displayed in the TFR maps in **Fig 3b**. Histograms are plotted below and to the right of the TFR to summarize the distribution of features in the respective domain. These histograms indicate the time points and frequency bins that are most important to the distinct neural traces of each task.

B. Classification Accuracy

Fig. 4a displays the classification confusion matrices for the traditional sensor-based and proposed source-based method averaged across the three subjects. The rows of the

confusion matrices represent the true identification of the trials and the columns represent the predicted identification of the trials. Therefore, the diagonal elements indicate the true positive rate (%) for each MI task. The off-diagonal elements of each row represent the false negative rate for any given MI task. Likewise, the off-diagonal elements of

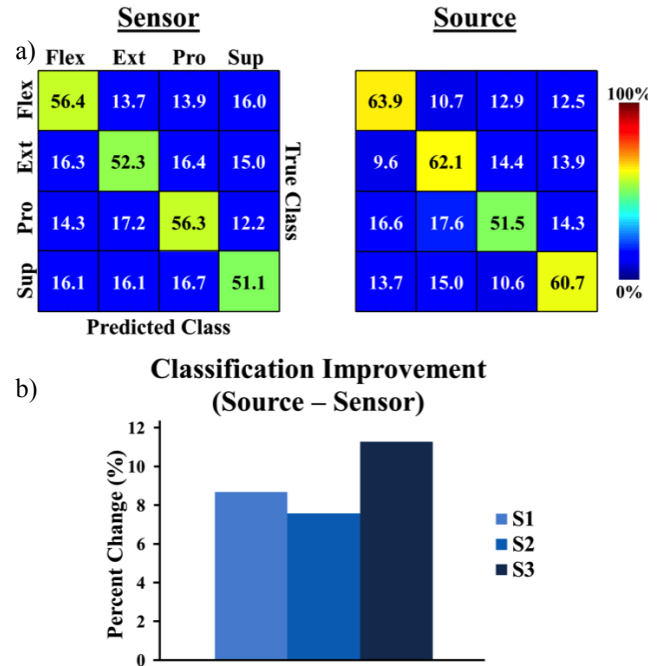


Fig. 4. (a) Averaged confusion matrices for sensor (left) and source (right) methods. The diagonal elements indicate the true positive rate (%) for each of the MI tasks. (b) Classification improvement (%) for each of the three subjects using source features compared to sensor features.

each column represent the false positive rate. For example, if a flexion trial were incorrectly classified as one of the other three tasks (false negative), this error would populate the respective block within the flexion row. On the other hand, if an extension, pronation or supination trial were incorrectly classified as a flexion trial (false positive), this error would populate the respective block of the flexion column.

The source-based method outperformed the traditional sensor-based method for three of the four individual MI tasks (flexion, extension and supination). The largest increase in performance for any one task was observed for extension with an increase of 9.8%. The source-based method displayed a decline in performance for only the supination task with a decrease of 4.8% compared to the sensor approach.

The grouped-averaged four-class classification accuracy for the sensor and source-based methods was 51.8% and 61.0% respectively, revealing a global increase of 9.2% for the proposed source-based method. **Fig. 4b** displays the subject-specific classification improvement for using source features compared to sensor features. Single subject improvement reached as high as 11.3%, resulting in an overall accuracy of greater than 65% in source space.

IV. DISCUSSION

In the present study, we have compared the use of ESI to traditional sensor-based methods for classifying four complex MI tasks of the right hand. Although much progress has been made in identifying useable MI tasks for high dimensional control of SMR BCIs, there is little realistic connection between the tasks being used and the action carried out by the end effector. MI tasks of the same limb present an opportunity to introduce systems that can carry out anthropomorphic commands using similar imaginations of one's own body parts. Our results from this pilot study demonstrate that separation of flexion, extension, supination and pronation is possible on the sensor level; however, is enhanced through the use of linear EEG inverse solutions.

To our knowledge, only [4] and [13] have attempted to separate the aforementioned MI tasks, in the sensor domain and source domain, respectively. These two studies primarily focus on binary classification schemes between pairwise combinations of the tasks and omit multi-class classification. Nevertheless, there was still an apparent increase in task separation using the ESI technique as compared to the traditional sensor-based method. Our results have displayed a similar trend of source-based features outperforming sensor-based features while applying more complex classification techniques.

The idea of motor cortex encoding has recently evolved into a theory of hierarchical networking where neuronal processes may be responsible for complex tasks rather than simply single muscle activation [14]. By constructing spatial feature maps within the right hand ROI (**Fig. 3a**) we were able to observe distinct distributions of discriminable information for each of the four tasks. These results indicate that the network activity of complex motor tasks may be preserved in scalp recorded data; however, is more

accessible when incorporating anatomical information through ESI techniques.

V. CONCLUSION

In addition to increasing the classification accuracy of flexion, extension, supination and pronation MI tasks over traditional sensor-based methods, the proposed ESI method allowed us to identify the network activity of these tasks in source space. In this sense, we were able to identify temporal-spectral-spatial biomarkers of each task that led to an increase in their separability. The results of this study are promising for integrating these four MI tasks into an online BCI for both recreational and rehabilitative purposes.

REFERENCES

- [1] A. J. Doud, J. P. Lucas, M. T. Pisansky, and B. He, "Continuous three-dimensional control of a virtual helicopter using a motor imagery based brain-computer interface," *PLoS One*, vol. 6, no. 10, Jan. 2011.
- [2] D. J. McFarland, W. A. Sarnacki, and J. R. Wolpaw, "Electroencephalographic (EEG) control of three-dimensional movement," *J. Neural Eng.*, vol. 7, no. 3, Jun. 2010.
- [3] B. He and L. Ding, "Electrophysiological Neuroimaging," in *Neural Engineering*, 2nd ed., B. He, Ed. Boston, MA: Springer US, 2013, pp. 499–543.
- [4] A. Vuckovic and F. Sepulveda, "Delta band contribution in cue based single trial classification of real and imaginary wrist movements," *Med. Biol. Eng. Comput.*, vol. 46, no. 6, pp. 529–39, Jun. 2008.
- [5] A. Vuckovic and F. Sepulveda, "Quantification and visualisation of differences between two motor tasks based on energy density maps for brain-computer interface applications," *Clin. Neurophysiol.*, vol. 119, no. 2, pp. 446–58, Feb. 2008.
- [6] A. K. Mohamed, T. Marwala, and L. R. John, "Single-trial EEG discrimination between wrist and finger movement imagery and execution in a sensorimotor BCI," in *Proceedings of the 33th Annual International IEEE EMBS Conference*, 2011, vol. 2011, pp. 6289–93.
- [7] L. Qin, L. Ding, and B. He, "Motor imagery classification by means of source analysis for brain-computer interface applications," *J. Neural Eng.*, vol. 1, no. 3, pp. 135–41, Sep. 2004.
- [8] B. Kamousi, A. N. Amini, and B. He, "Classification of motor imagery by means of cortical current density estimation and Von Neumann entropy," *J. Neural Eng.*, vol. 4, no. 2, pp. 17–25, Jun. 2007.
- [9] H. Yuan, A. Doud, A. Gururajan, and B. He, "Cortical imaging of event-related (de) synchronization during online control of brain-computer interface using minimum-norm estimates in frequency domain," *IEEE Trans. Neural Syst. Rehabil. Eng.*, vol. 16, no. 5, pp. 425–31, 2008.
- [10] F. Cincotti, D. Mattia, F. Aloise, S. Bufalari, L. Astolfi, F. De Vico Fallani, A. Tocci, L. Bianchi, M. G. Marciani, S. Gao, J. Millan, and F. Babiloni, "High-resolution EEG techniques for brain-computer interface applications," *J. Neurosci. Methods*, vol. 167, no. 1, pp. 31–42, Jan. 2008.
- [11] G. Pfurtscheller and L. Da Silva, "Event-related EEG/ MEG synchronization and desynchronization: basic principles," *Clin. Neurophysiol.*, vol. 110, no. 11, pp. 1842–57, 1999.
- [12] R. D. Pascual-Marqui, C. M. Michel, and D. Lehmann, "Low resolution electromagnetic tomography: A new method for localizing electrical activity in the brain," *Int. J. Psychophysiol.*, vol. 18, no. 1, pp. 49–65, Oct. 1994.
- [13] B. Edelman, B. Baxter, and B. He, "Discriminating hand gesture motor imagery tasks using cortical current density estimation," in *Proceedings of the 37th Annual International IEEE EMBS Conference*, 2014, pp. 1314–7.
- [14] M. Flanders, "Functional somatotopy in sensorimotor cortex," *Neuroreport*, vol. 16, no. 4, pp. 313–6, Mar. 2005.